CIRP Journal of Manufacturing Science and Technology 1 (2008) 70–75

Contents lists available at ScienceDirect

CIRP Journal of Manufacturing Science and Technology

journal homepage: www.elsevier.com/locate/cirpj

The influence of cutting edge sharpness on surface finish in facing with round nosed cutting tools

T.H.C. Childs [a,*], D. Dornfeld [b], D.-E. Lee [b], S. Min [b], K. Sekiya [c], R. Tezuka [c], Y. Yamane [c]

[a] School of Mechanical Engineering, University of Leeds, Leeds LS2 9JT, UK
[b] University of California at Berkeley, USA
[c] Hiroshima University, Japan

ARTICLE INFO

Article history:
Available online 31 October 2008

Keywords:
Precision
Machining
Surface
Finishing

ABSTRACT

The range of and particularly the minimum surface roughnesses achievable mainly with cemented carbide but also with single crystal diamond round nosed turning and facing inserts has been experimentally studied, machining aluminium and steel on engineering and precision lathes. Characteristic variations of machined surface profile with feed rate as well as insert edge sharpness and roughness measurements are reported. For aluminium faced by carbide inserts on precision lathes, insert edge radius (r_e) rather than feed marks determined R_z at low feeds, with $R_z \approx 0.02 r_e$. For steel work material, its properties rather than the insert edge radius became the R_z determining factor.

1. Introduction

Shaw and Crowell [1], in a seminal paper on surface finish from machining, contrasted finishes from the primary cutting edge, as are important in, e.g. plunge cutting and broaching, and from the secondary edge, as occurring in turning and facing, when feed marks are generated. The literature has, since then, mainly followed these divisions.

In primary edge studies, there has been a focus on edge geometry, particularly edge radius. The concept has emerged of a critical ratio of uncut chip thickness a_c to edge radius r_e, below which chip formation changes from cutting to ploughing dominated. Below the critical value, large increases in specific forces have been measured [2,3]. Changed surface appearances from clean cut to burnished have been reported [4,5]. Experimental and theoretical studies have indicated the critical value of a_c/r_e to be between 0.1 and 0.5, depending on material machined and cutting conditions [6,7]. But little has been reported on variation of surface roughness with a_c/r_e. Shaw's and Crowell's report that, at higher cutting speeds (in their experiments, above speeds at which built-up-edge was formed), peak-to-valley roughness was independent of feed remains one of the few relevant observations.

In secondary edge studies, researchers [1,4,8–16], machining ferrous and non-ferrous work materials with carbide, ceramic (PCD and PCBN) and single crystal diamond (SCD) tool inserts, report peak-to-valley roughnesses, e.g. R_z, close to kinematic values $f^2/(8r_n)$ at large feeds, where f is feed, r_n is tool nose radius. But as feed is reduced, R_z becomes independent of feed and may even increase as feed is further reduced. Fig. 1 brings together all the results. Given reasons for departure of roughness from kinematic values include machine tool limits (dynamic stiffness, feed control and bearing clearance effects), work material (it is responsible for process forces and how the chip separates from the work) and insert edge quality (its roughness along the edge and its radius in the plane normal to the edge). However, in contrast to the primary edge studies, only 3 of the 11 papers report edge radius values. None report on edge roughness.

But it is believed from the literature that typical edge radii r_e for cemented carbide inserts are in the range 10–20 μm and for SCD are around 0.1 μm. On this basis, the departures from kinematic roughness in Fig. 1, at around $f^2/[8r_n]$ from 2 to 8 μm for carbide and 0.02 to 0.08 μm for SCD inserts (or f^2/r_n from 16 to 64 and 0.16 to 0.64 μm, respectively), suggest a change in roughness determining mechanism at a ratio of f^2/r_n to r_e in the range ≈1–5. For round nosed tools (Fig. 2) f^2/r_n is also the value of uncut chip thickness a_c^* at point A along the cutting edge. a_c^* is the largest value of uncut chip thickness associated with the edge AB below which the residual work surface is generated [4]. Thus the data in Fig. 1 suggest a change of roughness determining mechanism at a value of a_c^*/r_e in the range 1–5. This is 10 times the 0.1–0.5 range of a_c/r_e from primary edge studies for a change from cutting to ploughing dominated material removal.

Fig. 1 may also be considered directly in terms of its minimum ranges of peak-to-valley height (2–8 μm for cemented carbide and

* Corresponding author.
E-mail address: t.h.c.childs@leeds.ac.uk (T.H.C. Childs).

1755-5817/$ – see front matter © 2008 CIRP.
doi:10.1016/j.cirpj.2008.09.001

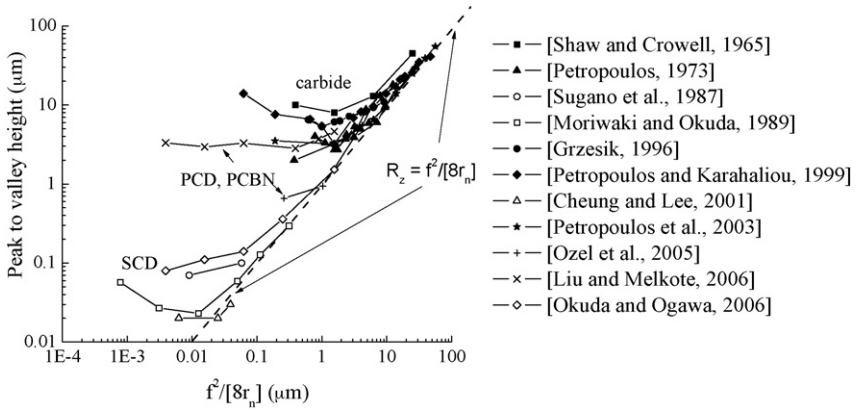

Fig. 1. Collected data on roughness from turning and facing with round nosed tools.

0.02–0.08 μm for SCD inserts). These are ≈0.1–0.5 r_e. The present paper investigates surface finish from the two perspectives, directly of the influence of r_e on R_z, and of the values of $f^2/[8r_n]$ at which departures from kinematic values occur. It reports new data on turning and facing aluminium and carbon steel with SCD and cemented carbide tools, on precision and general engineering machine tools, that suggest that the critical ranges of $f^2/[8r_n]$ and R_z in Fig. 1 are due to machine tool precision limits. For aluminium work, experimental conditions have been created for critical ranges to be associated with edge sharpness. Then the corresponding critical values of a_c^*/r_e do fall in the range 0.1–0.5. This work therefore creates a link between the two bodies of research, into finishes from primary and secondary cutting edges. Minimum values of R_z are found ≈$0.02r_e$. For steel work, its properties, perhaps microstructure, rather than r_e become the critical factor.

2. Experiments

1000 series aluminium and medium carbon steels were turned and faced in two different laboratories on complementary machine tools, using the same insert grades at both sites. Table 1 summarises. At Hiroshima, 100 mm diameter Al 1075 bar (HV 210 MPa) and normalised S45C steel (HV 1.4 GPa) were turned on a mechanically controlled engine lathe (10.2 kW Okuma, MT1 in Table 1) regarded as high precision for its class. 60 mm diameter discs from the Al bar were faced on a precision diamond turning machine (Toshiba Machine Co. ULC-100A, MT2). At Berkeley, 60 mm diameter discs cut from Al 1100 cold rolled plate (HV 420 MPa) and from AISI 1045 cold rolled steel bar (HV 2.4 GPa) were faced on a precision diamond turning machine (Rank Pneumo MSE-326, MT3) better protected against damage from overload than was the ULC machine. Cemented carbide and SCD insert tools were used. HTi10 (K grade, uncoated), UP20 M (TiN PVD coated) and UC5105 (Al_2O_3 on TiCN CVD coated) carbides were from Mitsubishi Carbide. T725X (multi-layer CVD coated) was from Toshiba Tungaloy. The SCD tools 1 and 2 were supplied by Sumitomo Electric Industries Ltd. SCD1 addressed the work with zero side and back rake angle. SCD2 was cut to present a large negative back rake to the work. It was claimed to be sharper than SCD1. The cemented carbide tools were used with side and back rakes of +5° (TP inserts) or −6° (CN inserts) at Hiroshima and +6° side rake, 0° back rake, at Berkeley.

With MT1, 20 mm lengths of bar were turned at feeds from 670 to 290 (depending on r_n) to 25 μm/rev. Then turning was always confined to inserts' nose radius regions. Cutting speed 200 m/min, depth of cut a_p 0.5 mm and no cutting fluid were used, after preliminary tests with Al 1075 and HTi10 inserts (speed 100–200 m/min; a_p 0.2, 0.5 mm; oil mist, dry) found negligible dependence of surface finish on these. Inserts were checked for tool wear with a low power microscope. If none was seen, the same corner continued to be used, otherwise a decision was made whether to change the corner.

With MT2 and MT3, 5–6 mm wide annuli were faced at feeds of 15, 10, 5, 2 (MT2) and 25, 10, 5 (MT3) μm/rev, adjusting spindle speeds to keep cutting speed in the range 200–100 m/min. a_p was varied between 5 and 2 μm, needed to limit cutting forces. Cutting fluid was used (oil mist MT2, methanol drip MT3), to aid swarf removal. Disc truing and subsequent tests over the range of feeds were carried out with a single insert corner, with a microscopic check for wear being made at the end. Problems that led to restricted cutting conditions for AISI 1045 on MT3 are described later.

The nose radius region edge radii r_e of the cemented carbide inserts were obtained by stylus profilometry. Inserts were held symmetrically in place beneath the stylus, with a corner to be measured at the highest point. The stylus was traversed perpendicular to the cutting edge, from the rake face to the relief face. A best circle was fitted to the raw data profiles. The edge radii of the SCD inserts were too small to be measured like this.

Cutting edge roughness was measured for the carbide inserts, traversing the stylus across the tool nose relief face, parallel to the

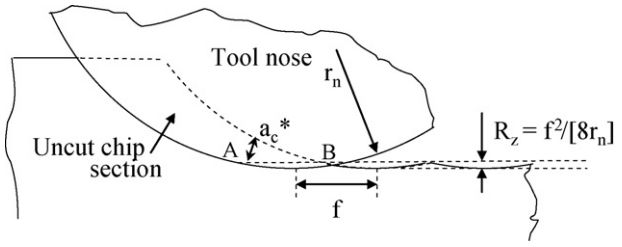

Fig. 2. Varying uncut chip thickness round the tool nose in turning and facing.

Table 1
Work, machine tool and insert combinations.

Work and machines				Insert description	r_e (μm)
Al 1075	Al 1100	S45C	AISI 1045		
MT1/2	MT3	MT1	MT3	HTi10 TPGN160304/08/16	6 ± 2
MT1	MT3	MT1	MT3	UP20M TPMN160308	55 ± 5
MT1	MT3	MT1	MT3	UC5105 TPMN160304	60 ± 5
MT1	–	–	–	T725X CNMG120408	80 ± 5
MT2	–	–	–	SCD1 r_n 0.5 mm	$<0.1_{nom}$
MT2	–	–	–	SCD2 r_n 0.5 mm	$<0.1_{nom}$

cutting edge and as close to the edge as could be judged. The data was used in two ways. It was used graphically to construct kinematic roughnesses of machined surfaces, taking roughness imperfections of the tool nose into account. Also, the nose radius form was removed from the data, followed by Gaussian filtering (upper cut-offs 250, 80, 25, 8, and 2.5 μm). Edge R_z values that resulted were also used as estimates of the machined surface kinematic peak-to-valley heights.

Workpiece height roughness parameters were measured. R_z (10 point height) is mainly reported here. Chart recordings were also made of the profiles. Different profilometers (stylus type unless otherwise described) were used for the tests on the MT1/2/3 machines, because of the machines' different locations. For MT1, a Kosaka Surfcorder SE-30D was used, with cutoff set at "R + W". For MT2, a Tokyo Seimitsu Accretech 3000A was used, with cut-off 0.25 mm. For MT3, a RTH Form Talysurf 120L and a white light interferometer (Wyko NT3300S) were used, both with cut-offs 0.25 mm. Comparisons between profilometers were made. Between-machine differences were similar to within-machine scatter except in one case (see later).

Work surface finish was also examined by scanning electron microscopy.

3. Results

Fig. 3 shows typical edge sharpness observations. The edge is not simply a circular blend from the rake to the flank. The opposed arrows show that the edge circle is inset in (a) from the flank and (b) and (c) from the rake face. In (b), the edge is closer to three segments than a circle. The edge radii in Table 1 are ranges from at least six corners. The values for the SCD inserts are from manufacturer's estimates.

Fig. 4a shows in its top left part, as an example, the cutting edge roughness round the tool nose of a UC5105 insert, scaled to the typical proportions at which work surface roughness traces are displayed. The remaining parts are kinematic roughnesses derived from this, by repeatedly indexing the insert profile 0.1, 0.05 and 0.025 mm, to create estimated work surface profiles at the feeds as marked. Fig. 4b plots R_z for the work surface roughnesses derived in this way from all the insert profiles (from visual inspection of peak-to-valley heights). It also shows the alternative estimates of R_z from Gaussian filtered insert roughness profiles. There is a reasonable agreement between the two methods. For the carbide inserts, the influence of edge roughness on R_z may be expected to exceed that of nose radius as feeds reduce below 0.05 mm/rev.

The measured roughnesses from cutting tests are shown in Fig. 5, for the MT1, and 6, for the MT2/3 tests. Fig. 5a shows results from turning Al 1075. No tool wear occurred, except for T725X at feeds less than 0.1 mm/rev. Then the relief face coating delaminated. For this insert there are two sets of data, unworn and worn (VB_{max} up to 0.26 mm). Because of its wear, T725X was not used further. Fig. 5a shows that at large feeds, R_z was from 1 to 2 times the kinematic roughness $f^2/[8r_n]$. At low feeds, R_z was independent of feed, ≈2–8 μm (in the absence of wear), the same for all inserts. Fig. 5b, with dashed lines from Fig. 5a, shows the same results from cutting S45C.

Fig. 6a shows Al, MT2/3, results. SCD1 and 2 facing Al 1075 on MT2 gave an optically good mirror finish at feeds ≤10 μm/rev, with R_z down to 60 nm. R_z from Al 1075 faced by HTi10 160304 on MT2 was of the same size, ≈0.2 μm at all feeds, as from Al 1100 faced by HiTi10 160304 and 160316 on MT3, except that measurements by white light interferometry from the 160304 insert used on MT3 were ≈0.1 μm. Apart from this, the data from HTi10 inserts establish an equivalence between facing Al 1075 on MT2 and Al 1100 on MT3. R_z from facing with UP20 M and UC5105 on MT3 was from 0.8 to 1.1 μm, also independent of feed.

It was not possible to carry out sustained cutting of steel on MT3, due to machine overload. Only the feed of 5 μm/rev was

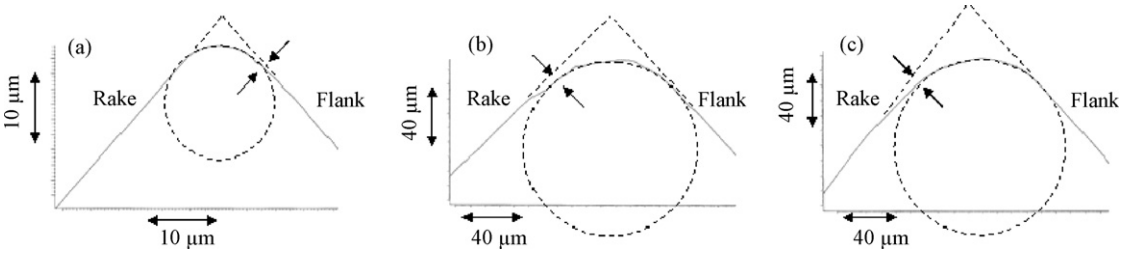

Fig. 3. Tool nose region cutting edge profiles: (a) HTi10, (b) UC5105, and (c) UP20 M.

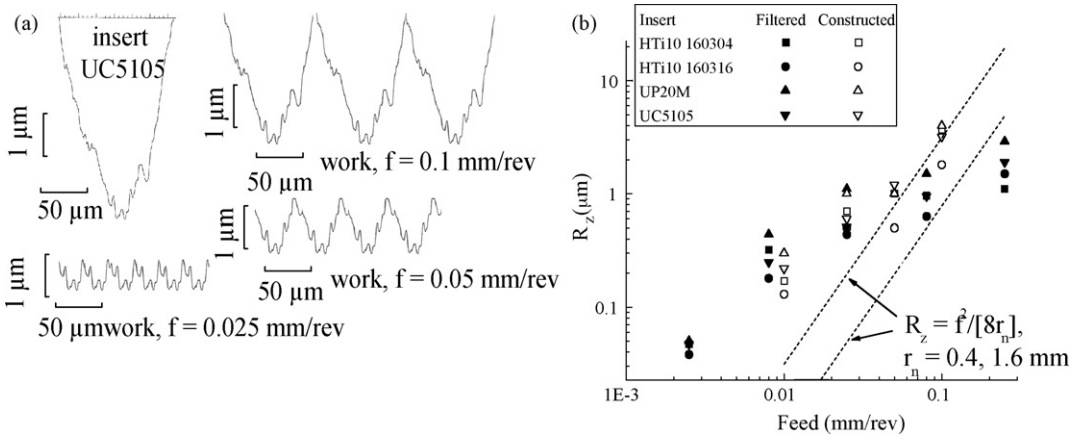

Fig. 4. (a) UC5105 cutting edge roughness and work surface kinematic roughness derived from it; (b) kinematic roughness estimates for all the inserts.

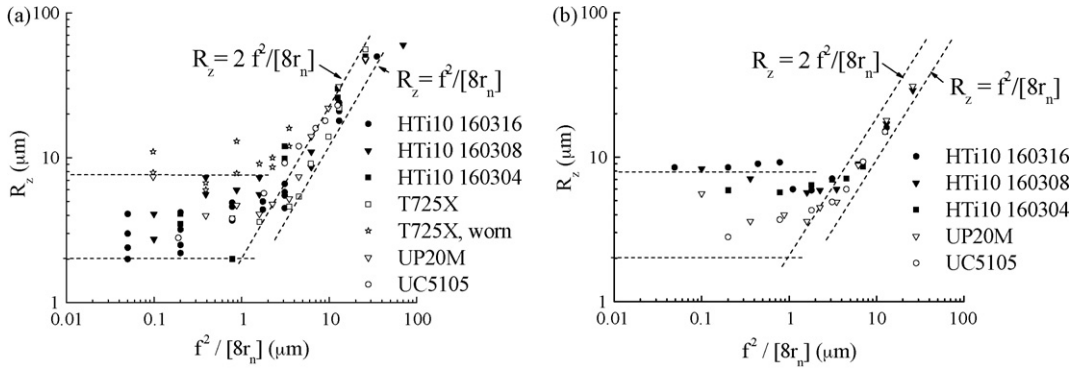

Fig. 5. R_z dependence on $f^2/[8r_n]$: (a) Al 1075 and (b) S45C faced on MT1.

achievable, and then for short periods of time, so that a maximum width of cut annulus was 1–2 mm. Even then, the UP20 M insert wore (VB_{max} = 0.15 mm). Faced surface roughness measurements showed greater differences between peak-to-valley height measures (e.g. R_t, R_z, R_{max}) than found for Al, so R_a was looked at too. Fig. 6b shows the dependence of R_z and R_a on r_e found for steel, compared to the Al data. R_a and R_z for steel were the same as for aluminium for r_e around 50–60 μm but hardly reduced at all as r_e reduced to 5–6 μm.

Fig. 7 shows aluminium work surface profiles from different feeds. Parts a and b, for which $f^2/[8r_n]$ = 7 and 0.4 μm, represent conditions (Fig. 5) where R_z (a) follows the kinematic trend and (b) is independent of feed. In (a) feed marks are deformed from their kinematic shape on their trailing faces, with height h 1.7 times the kinematic value; the observed R_z of up to twice the kinematic value (Fig. 5) is compatible with this. In (b) the profile has a wavelength twice the feed. Machine tool vibration would cause this. Parts c–e are from precision machining. (c) has a period of 15 μm, equal to the feed, and a wave form that might be expected from edge roughness (as in Fig. 3a). By the stage feed has reduced to 5 μm (part d), a less regular wave form is generated. For this surface, stylus profilometry gave R_z = 0.17 μm; observation of peak-to-valley heights over the 90 μm trace length of part d gives R_z closer to 0.1 μm. This is similar to the differences in R_z from stylus and white light machines. Finally part e is from facing with a SCD insert. $f^2/[8r_n]$ = 6 nm. Such a roughness is seen superimposed on an approximately square wave, amplitude 20 nm, wavelength 50 μm. As machine RPM was changed to maintain cutting speed constant, this wavelength remained unchanged. It is thus believed to arise from a MT2 feed drive imperfection.

Fig. 8 shows SEM views of surface finish from Al 1100 and AISI 1045 faced by HTi10 160304 and UC5105 inserts. For Al, non-groove-like features have widths across the feed marks of size equal to or less than the feed; for the HTi10 case (a), it was necessary to use a larger magnification than for UC5105 (b) to observe these. For the steel, the non-groove features tend to spread across several feed marks. These appear both as tears and deposits (white arrows in c and d).

4. Discussion

R_z reducing with to becoming independent of feed (Fig. 5) at $f^2/[8r_n] \approx$2–8 μm, machining with carbide inserts on an engineering lathe, is the same as in Fig. 1. That the transition and attainable roughness do not depend on edge radius nor work material points to their being determined by machine tool precision limits. A lower machine tool limit ($R_z \approx$60 nm) comes from facing with SCD inserts on a precision lathe (Fig. 6a).

New results from this work come from facing with carbide inserts on precision lathes. For aluminium (Fig. 6a) minimum R_z values have been independent of feed but dependent on edge radius. Surface imperfections from facing with HTi10 inserts are smaller than for UC5105 inserts (Fig. 8a and b). By plotting R_z against r_e (Fig. 6b) $R_z = 0.01–0.02r_e$. The same is true for steel faced by UC5105 and UP20 M inserts (Fig. 6b), but not by the HTi10 inserts. For the HTi10 inserts, larger R_z values are obtained with the steel than with the aluminium work. Fig. 8c and d suggest that finish is determined not by cutting edge radius but by work material behaviour, perhaps its ferrite/pearlite microstructure (etching showed pearlite colonies in the size range 20–100 μm) encouraging a larger stagnant zone under the cutting edge (though built-up-edge was not seen adhering to any of the inserts after cutting).

Carbide insert edge roughness (Fig. 4) could be expected to determine surface finish of aluminium over limited feed ranges

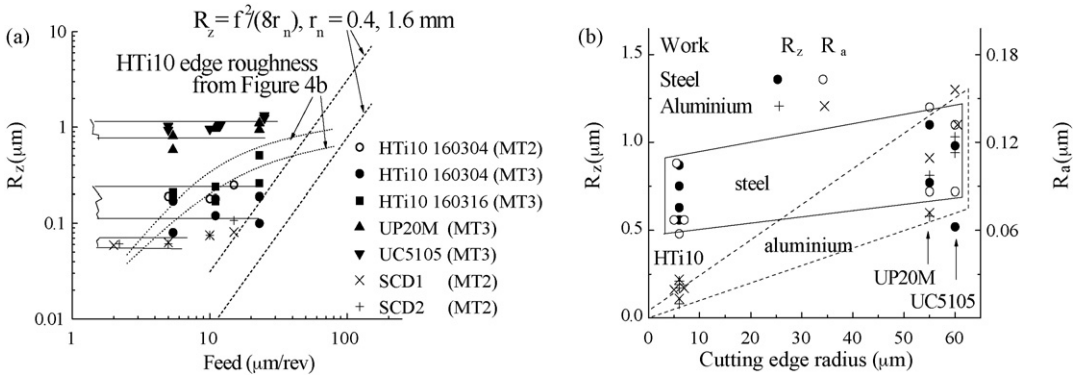

Fig. 6. (a) R_z vs. feed (Al, MT2/3); (b) R_z and R_a vs. r_e (Al, steel, f = 5 μm/rev).

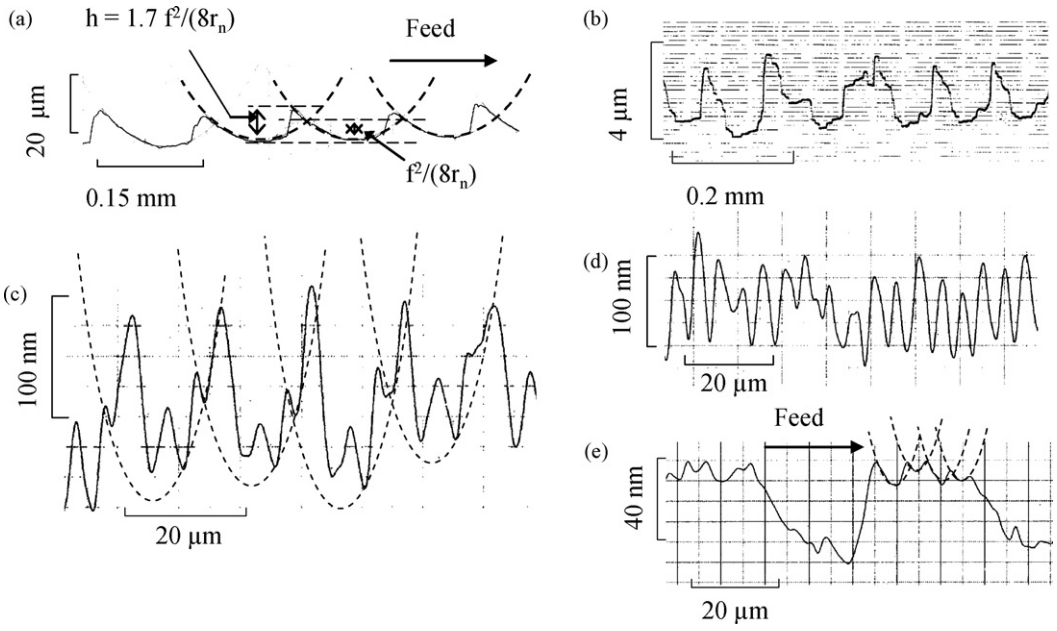

Fig. 7. Representative work surface profiles, all Al1075, at feed (μm/rev)/insert/MT sets: (a) 150/HTi10/1; (b) 50/HTi10/1; (c) 15/HTi10/2; (d) 5/HTi10/2; (e) 5/SCD/2.

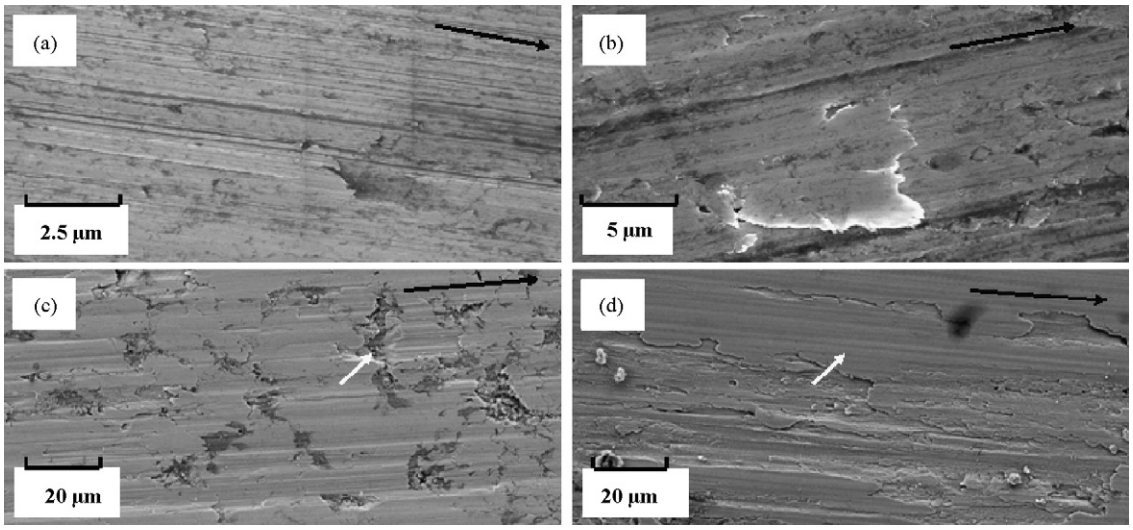

Fig. 8. Al (a and b) and steel (c and d) surfaces, f = 5 μm/rev, from HTi10 (a and c) and UC5105 (b and d) inserts, magnifications as marked (black arrows show insert sliding direction).

(from 0.05 mm/rev, Fig. 4b, down to feeds at which edge radius determines roughness). But in the present work (Al faced by HTi10 inserts) R_z less than that expected from edge roughness has been measured at f = 25 and 10 μm/rev. How the less than expected values arise is an open question. In Fig. 4b, the derived R_z values are proportional to $f^{1/2}$: this is as expected for a random rough surface [17] and reinforces the validity of methods to create the figure. The different R_z values from stylus and white light profilometry, for surfaces faced by the HTi10 160304 inserts, introduce an uncertainty into the true value. But even the upper estimate of ≈0.2 μm is less, at the feeds 25 and 10 μm/rev, than expected from Fig. 4b. Maybe the insert edge becomes effectively smoothed by a stable filling of its roughness valleys with work material.

From this paper's aluminium results, R_z caused by edge radius exceeds that caused by nose radius (feed marks) once $f^2/[8r_n] < (0.01–0.02)r_e$, or $f^2/[r_n r_e]$ (a_c^*/r_e from Section 1) < 0.08–0.16. This overlaps the range a_c/r_e from 0.1 to 0.5 from primary edge studies below which ploughing dominates chip formation. It may be argued from this that once feed marks become unimportant in determining roughness, then there is no difference between the secondary and primary edges as far as creation of surface finish is concerned. For steel faced by HTi10 inserts, the value of $f^2/[r_n r_e]$ below which feed marks become unimportant to the roughness rises to ≈0.5–1.0. This is above the 0.1–0.5 range. It would be of interest to study the finishes from other work materials.

5. Conclusion

When aluminium is turned/faced with round nosed cemented carbide inserts, its surface roughness changes from being insert nose to insert edge radius dependent as feed is reduced, unless machine tool precision limits intervene. $R_z = 0.01–0.02r_e$. This

leads to surface finish controlled by edge radius when $f^2/[r_n r_e] < 0.08–0.16$, which overlaps the range, from primary edge studies, of 0.1–0.5 when ploughing rather than cutting should dominate in the feed mark region of the chip/work interface. Perhaps at the low feeds at which feed marks no longer dominate surface finish in turning or facing, the processes determining finish are the same under the primary and secondary cutting edges. The results from facing a 0.45% carbon steel show a different behaviour: roughness determined perhaps by material's microstructure rather than by insert edge radius. It could be of interest for precision machining to study further what is and what controls the minimum roughness attainable with other work materials, with tools other than single crystal diamond, in the absence of machine tool limitations.

Acknowledgments

This work was supported by funding for visiting positions for one of us (THCC) from the Venture Business Laboratory of Hiroshima University and the Springer endowment of the University of California at Berkeley.

References

[1] Shaw, M.C., Crowell, J.A., 1965, Finish Machining, Annals CIRP, 13:5–22.
[2] Taminiau, D.A., Dautzenberg, J.H., 1991, Bluntness of the Tool and Process Forces in High-Precision Cutting, Annals CIRP, 40/1:65–68.
[3] Lucca, D.A., Seo, Y.W., 1993, Effect of Tool Edge Geometry on Energy Dissipation in Ultraprecision Machining, Annals CIRP, 42/1:83–86.
[4] Moriwaki, T., Okuda, K., 1989, Machinability of Copper in Ultra-Precision Micro Diamond Cutting, Annals CIRP, 381:115–118.
[5] Lucca, D.A., Seo, Y.W., Rhorer, R.L., 1994, Aspects of Surface Generation in Orthogonal Ultraprecision Machining, Annals CIRP, 43/1:43–46.
[6] Yuan, Z.J., Zhou, M., Dong, S., 1996, Effect of Diamond Tool Sharpness on Minimum Cutting Thickness and Cutting Surface Integrity in Ultraprecision Machining, Journal of Materials Processing Technology, 62:327–330.
[7] Liu, X., DeVor, R.E., Kapoor, S.G., 2006, An Analytical Model for the Prediction of Minimum Chip Thickness in Micromachining, Transactions of the ASME Journal of Manufacturing Systems and Engineering, 128:474–481.
[8] Petropoulos, P.G., 1973, The Effect of Feed Rate and of Tool Nose Radius on the Roughness of Oblique Finish Turned Surfaces, Wear, 23:299–310.
[9] Sugano, T., Takeuchi, K., Goto, T., Yoshida, Y., 1987, Diamond Turning of An Aluminium Alloy for A Mirror, Annals CIRP, 36/1:17–20.
[10] Grzesik, W., 1996, A Revised Model for Predicting Surface Roughness in Turning, Wear, 194:143–148.
[11] Petropoulos, G.P., Karahaliou, H., 1999, Investigating into the Effect of Small Feed Rate Values on the Roughness Produced by Turning Operations, in: Proceedings of the Third BALKANTRIB International Conference, vol. 1 (Sinaia, Roumania), pp.139–146.
[12] Cheung, C.F., Lee, W.B., 2001, Characteristics of Nano-Surface Generation in Single Point Diamond Turning, International Journal of Machine Tools & Manufacture, 41:851–875.
[13] Petropoulos, G.P., Torrance, A.A., Pandazosas, C.N., 2003, Abbott Curve Characteristics of Turned Surfaces, International Journal of Machine Tools & Manufacture, 43:237–243.
[14] Ozel, T., Hsu, T.-K., Zeren, E., 2005, Effects of Cutting Edge Geometry, Workpiece Hardness, Feed Rate and Cutting Speed on Surface Roughness and Forces in Finish Turning of Hardened AISI H13 Steel, International Journal of Advanced Manufacturing Technology, 25:262–269.
[15] Liu, K., Melkote, S.N., 2006, Effect of Plastic Side Flow on Surface Roughness in Micro-Turning Process, International Journal of Machine Tools & Manufacture, 46:1778–1785.
[16] Okuda, K., Ogawa, E., 2006, Study on Step at Grain Boundary in Ultra-Precision Cutting of Phosphor Bronze, in: Proceedings of Eighth ICTMP, JSPE, Japan, pp. pp.393–396.
[17] Thomas, T.R., 1982, Rough Surfaces, Longman, New York. pp. 116–117.